

THE LOW-FREQUENCY DIELECTRIC RESPONSE AND NON-LINEAR DC ELECTRICAL TRANSPORT IN κ -(BEDT-TTF)₂Cu[N(CN)₂]Cl

Marko Pinterič^{1,2*}, Neven Biškup¹, Silvia Tomić¹, Dieter Schweitzer³,
Werner Strunz⁴, Ilisabe Heinen⁴

¹Institute of Physics, P. O. Box 304, 10000 Zagreb, Croatia,

²Faculty of Civil Engineering, University of Maribor, Slovenia,

³3. Physikalisches Institut, Universität Stuttgart, Germany,

⁴Anorganisch-chemisches Institut, Universität Heidelberg, Germany

ABSTRACT: We report AC transport and non-linear DC electrical transport in single crystals of the organic conductor κ -(BEDT-TTF)₂Cu[N(CN)₂]Cl. Non-linear conductivity emerges below 22 K, which is the temperature of canted antiferromagnetic ordering. A broad dielectric relaxation mode of moderate strength ($\Delta\varepsilon \sim 3 \times 10^3$) appears at 32 K, and weakens with temperature. The mean relaxation time, much larger than that expected for single-particle excitations, is thermally activated in a manner similar to the DC conductivity and saturates below 22 K. The observed dielectric response data give evidence of a collective mode contribution to the dielectric properties, which might be attributed to charged domain walls in a ferromagnetic domain structure. Non-linear conductivity similar to those observed for commensurate spin and charge density waves are found.

1. INTRODUCTION

One family of novel organic metals that received special interest in recent time is κ -(BEDT-TTF)₂Cu[N(CN)₂]X family, where BEDT-TTF is Bis(ethylenedithio) tetrathiafulvalene and X is a halogenide. That is, when substituting X for Br, the ground state is superconducting with the highest superconducting critical temperature among organic metals. On the other side, substituting X for Cl leads to semiconducting material with the canted antiferromagnetic ground state. Moreover, when subjected to the pressure of only 300 bars [1], the latter material undergoes a transition to superconducting state. In this case we face a competition between superconducting and antiferromagnetic states, which is also interesting for theoretical understanding of superconductivity. Here we present for the first time a complete account of the collective conduction properties of κ -(BEDT-TTF)₂Cu[N(CN)₂]Cl material.

κ -(BEDT-TTF)₂Cu[N(CN)₂]Cl material belongs to the κ -(BEDT-TTF)₂X (X is polymerised anion) class of BEDT-TTF systems in which orthogonally aligned BEDT-TTF dimers form 2D conducting layers sandwiched between the polymerised anion layers. Its unit cell contains two BEDT-TTF layers (*i.e.* 4 dimers) and 4 anions [2]. The donor molecules form face-to-face orthogonal dimers which are rotated by circa 45 degrees with respect to the unit cell axes (*a* and *c*). The copper atoms complete their trigonal coordinate ion environment with a bond to a terminal chlorine atom. The 2D layers of the organic donor molecules lie in the crystallographic *ac* plane, which

* e-mail: mpinter@ifs.hr

coincides with the large face of the crystal, and these layers are alternatively separated by anion layers along the b axis.

Overlap between BEDT-TTF molecules leads to formation of two-dimensional band and strong anisotropy between in-plane and out-of plane conductivity. No anisotropy in in-plane electronic characteristics larger than a factor of 2 was found. Since we have one electron per one dimer (that is one electron per two BEDT-TTF molecules) and quarter-filled band, we expect ordering of periodicity $N = 4$. All conductivity properties were measured within the ac plane.

2. MAGNETIC PROPERTIES

The results of NMR measurements of Miyagawa *et al.* [3] showed a large enhancement of the spin-lattice relaxation rate below 50 K and a sharp peak at 27 K. The former was interpreted to be due to the antiferromagnetic spin fluctuations, and the latter as a sign of an antiferromagnetic phase transition. The established order is commensurate with the underlying lattice and possesses a rather large moment of (0.4-1.0) μ_B per dimer. In addition, magnetisation measurements by the same authors showed that weak ferromagnetism appears below 23 K due to the canting of spins. As in this temperature range a finite energy gap is already opened in the charge degrees of freedom, Miyagawa *et al.* suggested that the magnetic ordering of localised spins driven by electron-electron correlations was in origin of the observed phase transition.

To get more information about the low-temperature state, we have performed measurements of the magnetic anisotropy using torque method [4]. Temperature dependant susceptibility anisotropy and especially appearance of spin-flop effect below 22 K have given clear evidence of a canted antiferromagnetic state established below 22 K, with the easy axis in the direction of b axis. Besides that, the angular dependent susceptibility anisotropy in bc plane has revealed that the vector of ferromagnetic magnetization is directed along c axis. The size of ferromagnetic effect corresponds to situation in which 1/1000 of total number of spins would arrange in ferromagnetic manner. That correspond to the canting of all spins for 6×10^{-2} degrees from b axis. We have suggested that the features observed could be accounted for taking into consideration the Dzyaloshinsky-Moriya interaction. In a two-sublattice model of antiferromagnetism, such an interaction will cant the sublattices toward one another and hence create a weak magnetic moment of the order of $|\mathbf{D} \cdot (\mathbf{M}_1 \times \mathbf{M}_2)|$. \mathbf{M}_i is the static sublattice magnetization, and \mathbf{D} is a constant vector. This argument was supported by symmetry considerations. Finally, the hysteresis of the order 1 kOe in the spin-flop transition and magnetic field reversal of the ferromagnetic magnetisation are features not encountered in the standard antiferromagnets and spin density waves. The latter feature indicates the existence of a domain structure, which is a well-known property of magnetically ordered state. That is, when the magnetic field is absent the energy of the ferromagnetic crystal is lowered when the crystal is divided into domains with equivalent spin configurations.

3. ELECTRICAL PROPERTIES

We report results obtained on three different crystals. All crystals have showed the same properties. Their room temperature (RT) conductivity has been about 5 Scm^{-1} . The ohmic and non-ohmic resistivity have been measured in the four probe

configuration using a standard DC technique. The complex admittance ($G(\omega)$, $B(\omega)$) has been measured by a Hewlett Packard HP4284A impedance analyser (20Hz-1MHz) in the two probe configuration in the temperature range between 7K and 40K. Dielectric functions have been extracted from the conductivity using relations $\epsilon'(\omega)=B(\omega)/\omega$, and $\epsilon''(\omega)=(G(\omega)-G_0)/\omega$, where G_0 is DC conductivity obtained from measured $G(\omega)$ at low frequencies where $G(\omega)$ was independent of ω .

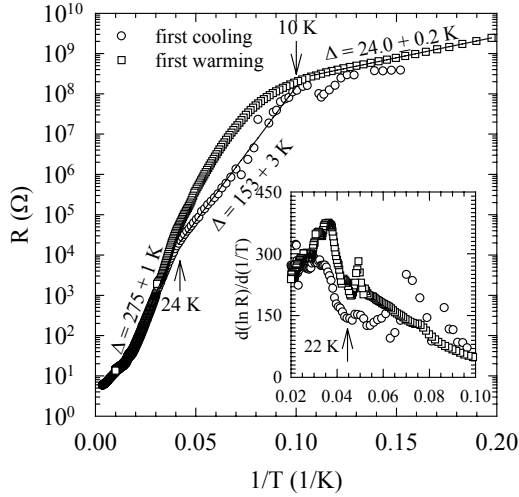


Figure 1: Resistivity and gap width (Inset) *versus* inverse temperature. The fits represent Arrhenius behaviour.

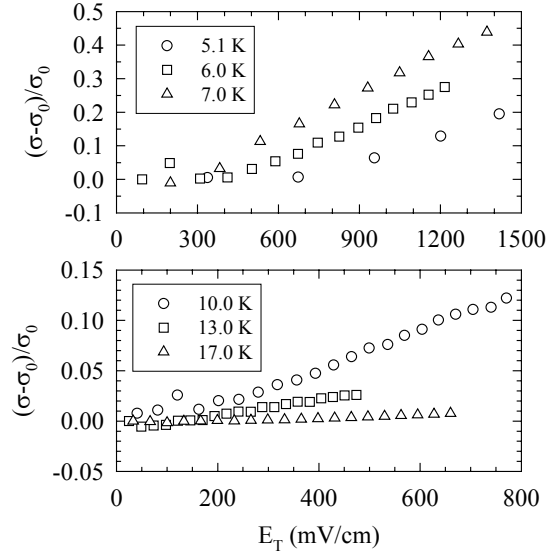


Figure 2: Non-ohmic conductivity *versus* electric field at few typical temperatures.

Resistance as the function of inverse temperature is shown in Figure 1. Resistivity follows semiconducting (Arrhenius) behaviour and the gap width $d(\ln R)/d(1/T)$ changes with the temperature (see Inset). On first cooling, the gap width below 50 K is about 275 K and then it abruptly changes to 153 K below 22 K. On first warming and also on subsequent temperature cycles, the change is no longer sharp and gap width changes continuously. This might not be surprising, since we have already reported changes in some magnetic properties of the sample with thermal cycling in the high temperature range [4].

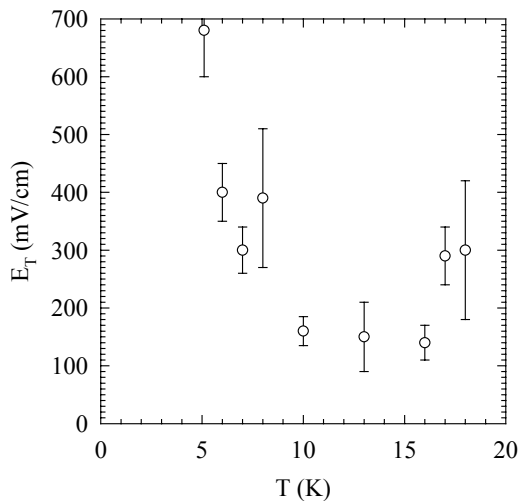


Figure 3: Threshold electrical field *versus* temperature.

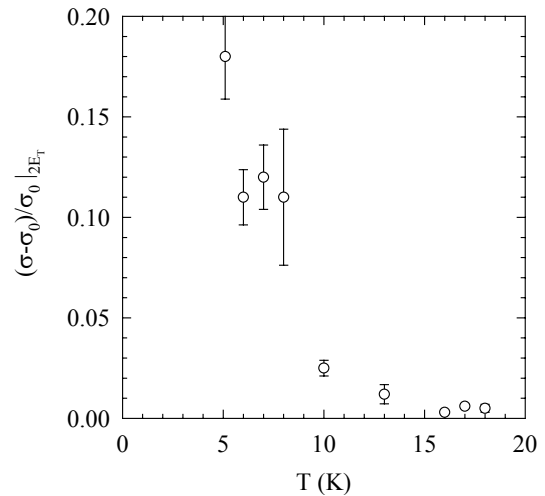


Figure 4: Non-ohmic conductivity at two threshold electrical field, normalised to its ohmic value, *versus* temperature.

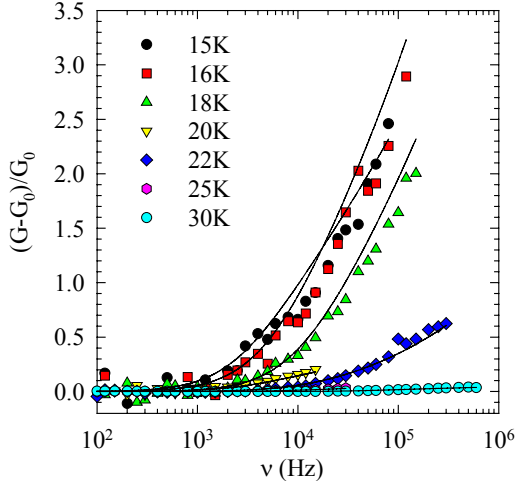


Figure 5: Real part of the conductivity normalised to the DC value versus frequency for temperature range between 30 K and 15 K. Full lines are fits to HN form.

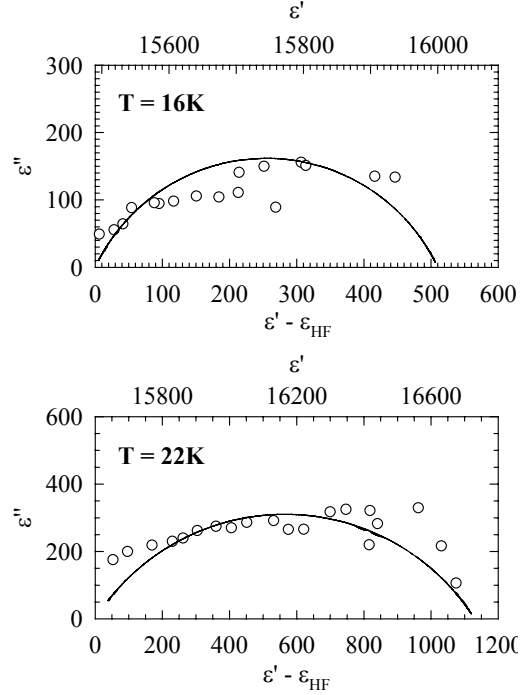


Figure 6: Cole-Cole plots of the dielectric response at two selected temperatures. Full lines are fits to the HN form.

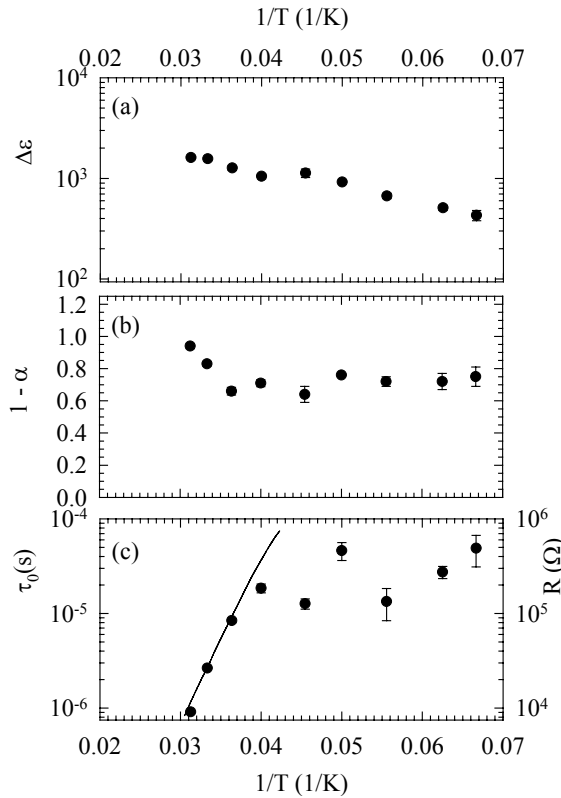


Figure 8: (a) Relaxation strength, (b) shape parameter, (c) mean relaxation time (full points) and DC resistance (full line) versus inverse temperature.

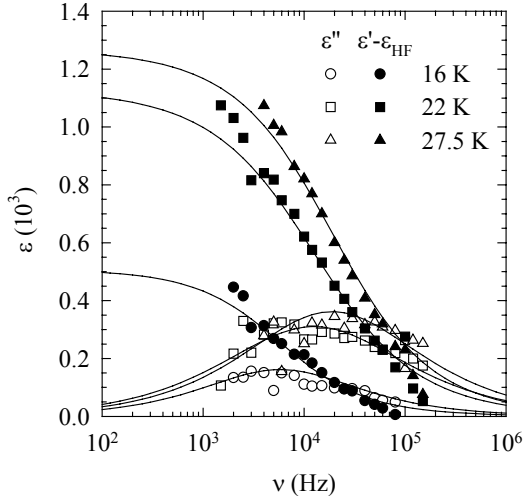


Figure 7: Frequency dependence (log scale) of the real and imaginary parts of the dielectric function for three representative temperatures. Full lines are fits to the HN form.

Figure 2 shows the field-dependent conductivity normalised to its ohmic value at a few selected temperatures. Above a certain threshold electrical field, E_T , conductivity starts to increase, since the additional, collective conducting channel opens. The magnitude of non-linear conductivity is negligible above 12 K, as shown in Figure 4. Below that temperature it increases concomitantly with the rise of the threshold electrical field (see

Figure 3). This behaviour is somewhat surprising. That is, the increase of threshold field suggests that the sliding mechanism starts to freeze below 12 K. In that case one would expect concomitant decrease of non-linear conductivity as reported in commensurate charge density wave system [5]. However, such unexpected behaviour was also observed in the system with commensurate spin density wave [6].

The real part of the conductivity normalised to the DC value $(G(\omega)-G_0)/G_0$ as a function of frequency at a few selected temperatures between 15 K and 30 K is shown in Figure 5 [4]. At $T > 32$ K a frequency independent conductivity is found. Note that an enhanced AC conductivity grows in importance and starts at lower frequencies as the temperature lowers. The initial analysis of the dielectric function was performed by the inspection of Cole-Cole plots, which are presented in Figure 6. The intersection of the arcs with ϵ' axis at high and low ϵ' values, corresponding to low and high frequencies, indicates the values of the static dielectric constant ϵ_0 and the high frequency dielectric constant ϵ_{HF} , respectively. The value of the relaxation strength $\Delta\epsilon = \epsilon_0 - \epsilon_{HF}$ is moderate, of the order of 1000. Figure 7 shows frequency domain plots of the real and imaginary part of the dielectric function at three selected temperatures. It should be noted that $\epsilon''(\nu)$ curves move toward lower peak frequencies ($\nu_0 = \omega_0/2\pi = 1/2\pi\tau_0$) and smaller peak amplitudes with decreasing temperature without significant change in the shape.

Detailed analysis of the collective mode was made in terms of the complex dielectric function $\epsilon(\omega)$ given by a generalisation of the Debye expression known as the phenomenological Havriliak-Negami (HN) function [7]

$$\epsilon(\omega) - \epsilon_{HF} = \Delta\epsilon \frac{1}{[1 + (i\omega\tau_0)^{1-\alpha}]^\beta} \quad (1)$$

where $\beta = 1$ for symmetrical cases. τ_0 and $1-\alpha$ are the mean relaxation time and the shape parameter, which describes the symmetric broadening of the relaxation time distribution function, respectively.

The full lines in Figures 5, 6 and 7 correspond to the calculated fits. The fit parameters as a function of inverse temperature are shown in Figure 8. The parameter $\Delta\epsilon$ corresponds to the static dielectric susceptibility and decreases with temperature less than one order of magnitude between 32 K and 14 K. The width of the relaxation time distribution expressed by the $(1 - \alpha)$ parameter is close to 1 at 32 K. However, already below 28 K the mode broadens and the value of $(1 - \alpha) \sim 0.7$ does not change significantly with temperature. The mean relaxation time τ_0 closely follows the thermally activated behaviour in a manner similar to the DC conductivity in the temperature range 32 K – 25 K, and saturates below 22 K.

4. DISCUSSION

The dielectric relaxation appears below 32 K. The width is larger than for the Debye process and does not change with temperature below 28 K. The relaxation strength is of the order of 1000 and decreases on lowering the temperature. The characteristic relaxation time is too long to be attributed to free carriers. τ_0 is thermally activated with the activation energy close the free-carriers one in the narrow temperature range 32 K – 25 K and saturates below $T_N = 22$ K. Therefore, we are led to identify the origin of this

relaxation as an intrinsic property of the weak ferromagnetic state established below 22 K. We propose a charged domain wall in the ferromagnetic domain structure as the relaxation entity. The broad distribution of relaxation times $(1 - \alpha) \sim 0.7$ might be reasonably assumed to be due to a distribution of activation energies. Then, the dielectric response is due to the activation between different metastable states over energy barriers. These metastable states correspond to local changes of the spin configuration. The length scale over which such processes occur defines the thickness of the wall and is set by the competition between relevant energies of the problem. The fact that the energy scale for the barrier heights is close to the free-carrier activation energy only above $T_N = 22$ K indicates that the free-carrier screening influences the relaxation only in the fluctuating pretransitional regime. At 22 K the relaxation time levels off. The change in the $\log \tau_0$ versus $1/T$ plot at $T_N = 22$ K might indicate that the resistive dissipation is not the dominant dissipation mechanism in the weak ferromagnetic state. That is, one could expect that the free-carrier screening becomes unimportant once the electron density becomes smaller than the one electron per the domain wall length L_{WF} . If we assume that this condition is satisfied at $T < 20$ K and take into account the resistance increase of about 5 orders of magnitude between RT and 20 K, we get for $L_{WF} \sim 100 \mu\text{m}$. As far as the temperature behaviour of the relaxation strength is concerned, a observed decrease might indicate that the domain walls are more restricted to move as the temperature lowers.

The behaviour of non-ohmic conductivity, similar to previously observed properties of commensurate spin density waves remains unclear. Our results demonstrate that electrons are not localised to a degree in which collective mode response to the DC electric field would be disabled. However, no theory so far satisfactory explains the sliding of collective mode in situation where screening of free electrons disappears. More investigation in this direction is necessary.

5. REFERENCES

- [1] J.M. Williams et al., "Form Semiconductor-Semiconductor Transition (42 K) to the Highest- T_C Organic Superconductor κ -(ET) $_2$ Cu[N(CN) $_2$]Cl ($T_C = 12.5$ K)", *Inorg. Chem.* **29**, (1990) 3272.
- [2] J.M. Williams et al., *Organic Superconductors*, Prentice Hall, Englewood Cliffs, 1992, ISBN 0-13-640566-5.
- [3] K. Miyagawa, A. Kawamoto, Y. Nakazawa and K. Kanoda, "Antiferromagnetic Ordering and Spin Structure in the Organic Conductor, κ -(BEDT-TTF) $_2$ Cu[N(CN) $_2$]Cl", *Phys. Rev. Lett.* **75**, (1995) 1174.
- [4] M. Pinterić, M. Miljak, N. Biškup, O. Milat, I. Aviani, S. Tomić, D. Schweitzer, W. Strunz and I. Heinen, "Magnetic anisotropy and low-frequency dielectric response of weak ferromagnetic phase in κ -(BEDT-TTF) $_2$ Cu[N(CN) $_2$]Cl, where BEDT-TTF is Bis(ethylenedithio)tetrathiafulvalene", *Eur. Phys. J. B* **11** (1999) 217.
- [5] M. Pinterić, N. Biškup, S. Tomić, J.U. von Schütz, "Non-ohmic electrical transport in the charge-density wave state of (2,5(OCH $_3$) $_2$ DCNQI) $_2$ Li", *Synth. Metals* **103**, (1999) 2185.
- [6] S. Tomić, N. Biškup, S. Dolanski Babić and K. Maki, "Commensurate Spin-Density Wave State in (TMTTF) $_2$ Br: Single-Particle and Collective Charge Dynamics", *Europhys. Lett.* **26**, (1994) 295.
- [7] R.J. Cava, R.M. Fleming, R.G. Dunn and E.A. Rietman, "Low-frequency dielectric response of the charge-density wave in orthorhombic TaS $_3$ ", *Phys.Rev.B* **31** (1985), 8325.